Microporous and Mesoporous Materials 209 (2015) 90–98

Contents lists available at ScienceDirect

Microporous and Mesoporous Materials

journal homepage: www.elsevier.com/locate/micromeso

Temperature dependence of the electrical conductivity of activated carbons prepared from vine shoots by physical and chemical activation methods

A. Barroso-Bogeat [a,*], M. Alexandre-Franco [a], C. Fernández-González [a], A. Macías-García [b], V. Gómez-Serrano [a]

[a] Department of Organic and Inorganic Chemistry, Faculty of Sciences, University of Extremadura, Avda. de Elvas s/n, E-06006 Badajoz, Spain
[b] Department of Mechanical, Energetic and Materials Engineering, University of Extremadura, Avda. de Elvas s/n, E-06006 Badajoz, Spain

ARTICLE INFO

Article history:
Received 13 May 2014
Accepted 15 July 2014
Available online 23 July 2014

Keywords:
Vine shoots
Activated carbon
Electrical conductivity
Energy gap

ABSTRACT

A broadly varied series of activated carbons (ACs) was prepared from vine shoots (VS) by the method of physical activation in air, CO_2 and steam, and by the method of chemical activation with H_3PO_4, $ZnCl_2$ and KOH aqueous solutions. Here, the temperature dependence of the dc electrical conductivity for the ACs is studied from room temperature up to 200 °C. The bulk electrical conductivity of the carbon samples is found to be the result of a complex interplay between several factors, texture and surface chemistry likely being the most relevant ones. The best conductivity values are obtained for sample carbonized at 900 °C. The physical activation stage has been proved to decrease the conductivity of the carbonized products, the reduction being more pronounced for air than for CO_2 and steam. Such a detrimental effect of physical activation on conductivity has been associated with the formation of oxygen groups and structures on carbon surface rather than with the porosity development. The conductivity of ACs prepared by chemical activation is even lower than for physically activated samples, likely due to the higher degree of porosity development. All carbon samples, irrespective of the activation method and activating agent, behave as semiconductor materials and therefore the electrical conduction is related to an energy gap (E_g). The E_g values widely vary from 0.084 eV for the sample carbonized at 900 °C up to 0.659 eV for the AC prepared by physical activation in air.

1. Introduction

Activated carbon (AC, hereafter) is an amorphous carbon material characterized by its excellent textural properties (i.e. surface area, porosity and pore size distribution) and surface chemistry. It is well-known that these properties of AC strongly depend on the raw material and the method employed in its preparation process [1–4], including the activating agent as well as the operational conditions. A great variety of precursors with high carbon content and low amount of inorganic compounds are widely used in the large-scale manufacture of AC, such as woods, coals, lignite, coconut shell, peat, fruit stones, polymers, and so on [1,3,5–8]. Nowadays, the production of ACs from industrial and agricultural waste products is an issue of active research, with a view not only to their controlled removal and valorization but also to prepare lower-cost ACs [9].

Vine shoots (VS, henceforth) are an agricultural waste generated in most of the European Mediterranean countries as a result of the pruning works carried out yearly in all vineyards after the grape harvest. The annual production of VS in Spain is in the order of several million tons [10], and such an amount has been estimated to be at around 87,725 tons only for the Autonomous Community of Extremadura (south-west Spain) [11,12]. Because of their low density and thereby high transportation cost, the valorization of VS is a very difficult task and as a result they are usually burnt in the open air with release of greenhouse effect gases. This solution is the fastest one but not the best one, both from economic and environmental standpoints. As a way of diversifying the applications of this agricultural residue and increasing its profitability, some previous works have shown that VS are an attractive precursor for the preparation of ACs [9,13–15], which have been successfully applied in the removal of dyes from water streams [16] and in the wine treatment [17].

AC has a wide range of applications, including water treatment, gas separation and storage, removal of pollutants by adsorption

* Corresponding author. Tel.: +34 924 289421; fax: +34 924 271449.
E-mail address: adrianbogeat@unex.es (A. Barroso-Bogeat).

http://dx.doi.org/10.1016/j.micromeso.2014.07.023
1387-1811/

both from liquid and gaseous effluents, solvent recovery, in heterogeneous catalysis acting either as catalyst by itself or more commonly as catalyst support, in electrocatalysis, sensors and actuators, and so on [1–3,18]. Recently, special attention has been focused on the use of AC as electrode material in electrical energy storage devices, mainly supercapacitors [19–28] and lithium ion batteries [29–33]. Among other factors (specific surface area, pore size distribution, chemical and thermal stability, presence of electroactive surface functional groups and structures, electrolyte, and so forth [22,24,34,35]), electrical conductivity has been shown to play a major role on the potential application and performance of ACs in the aforesaid devices [36,37]. On the other hand, the properties of the carbon support, especially its electrical conductivity, largely determine the electrochemical performance of carbon-based electrocatalysts [38]. Therefore, it becomes apparent that the measurement of the electrical conductivity of ACs at different temperatures is essential in order to assess some of their potential applications. Moreover, based on a previous literature review, the influence of the preparation process of AC (i.e. activation method and activating agent) on its electrical behavior over a wide temperature range has not been reported yet. In fact, we only found a few papers concerning the analysis of the temperature-dependent electrical conductivity for ACs prepared from coconut shell [39] and rice husk [40] by chemical activation with KOH and H_3PO_4, respectively, and from Kapton® films [41] and rayon [42] by physical activation in CO_2 and steam.

In the present work, the temperature dependence of the dc electrical conductivity is studied for a broadly varied series of ACs, which were previously prepared from VS by physical and chemical activation methods and characterized elsewhere [9]. Thus, the influence of both the activation method and the activating agent on the conductivity and electrical behavior of the ACs is investigated. The systematic use of complementary techniques for the chemical, textural and electrical characterization of the materials reveals the general trends in the electrical properties of the VS derived-ACs.

2. Experimental

2.1. Raw material

The VS (*Vitis vinifera* variety) used in the present study were grown and collected in a vineyard located in the wine-producing region named Tierra de Barros (Badajoz province, south-west Spain). The as-received VS were air-dried, size-reduced and sieved, the fraction of particle sizes lower than 1 mm being selected for the subsequent preparation of the various ACs.

2.2. Preparation and characterization of the ACs

The preparation of the ACs was carried out following the methods described in detail by Ruíz-Fernández et al. [9,16], which are summarized in Table 1 together with the codes assigned to the resulting products. The textural characterization of the ACs was accomplished by N_2 adsorption at −196 °C, mercury porosimetry, and helium and mercury density measurements. The specific surface area (S_{BET}) was estimated by applying the Brunauer, Emmet and Teller equation [43] to the experimental N_2 isotherms. The theoretical background for microporosity characterization was based on Dubinin's theory. Thus, the analysis of the adsorption isotherms by the Dubinin–Radushkevich (D–R) equation led to the values of the micropore volume (W_0) [44]. The mesopore (V_{me}) and macropore (V_{ma}) volumes were derived from the mercury intrusion curves. Finally, the total pore volume (V_T') was calculated from W_0, V_{me} and V_{ma}. These textural data for the prepared ACs have been previously reported elsewhere [9], and are collected in Table 2.

The surface functional groups and structures of the ACs were qualitative and quantitative analyzed by FT-IR spectroscopy and Boehm's method [45], respectively. Using a Perkin Elmer® 1720 spectrometer, the spectra were recorded between 4000 and 400 cm^{-1}, with 50 scans being taken at 2 cm^{-1} resolution. Pellets were prepared by first size-reducing a certain amount of the ACs

Table 1
Methods of preparation and sample codes for ACs.[a]

Substratum	Mass (g)	Atmosphere; AA	Flow (mL min^{-1}); AA:VS ratio	MHTT (°C)	t (h)	Code
VS	10	N_2	80	600	2	C600
VS	10	N_2	80	900	2	C900
C600	1.5	Air	10	275	1	A
C900	1.5	CO_2	10	750	1	CD
C900	1.1	N_2-steam	80 (N_2)	750	1	S
VS	25	H_3PO_4	5:1	85	2	PA-IP
VS	25	$ZnCl_2$	5:1	85	7	ZC-IP
VS	25	KOH	2:1	85	2	PH-IP
PA-IP	10	N_2		500	2	PA
ZC-IP	10	N_2		500	2	ZC
PH-IP	10	N_2		800	2	PH

[a] Abbreviations: VS, vine shoots; AA, activating agent; MHTT, maximum heat treatment temperature; t, isothermal time at MHTT.

Table 2
Textural parameters of the ACs.

Sample	S_{BET} (m^2 g^{-1})	W_0 (cm^3 g^{-1})	V_{me} (cm^3 g^{-1})	V_{ma} (cm^3 g^{-1})	V_T'[a] (cm^3 g^{-1})
C600	34	0.010	0.07	0.54	0.62
C900	5	0.001	0.08	0.38	0.46
A	322	0.16	0.03	0.58	0.77
CD	293	0.14	0.07	0.41	0.62
S	572	0.26	0.17	0.69	1.12
PA	1363	0.48	0.69	0.47	1.64
ZC	1726	0.59	0.81	0.37	1.77
PH	791	0.37	0.07	1.13	1.57

[a] $V_T' = W_0 + V_{me} + V_{ma}$.

for homogenization and then accurately weighing a mass of the ground product, which was thoroughly mixed with KBr at the 1:500 AC/KBr weight ratio in a small size agate mortar. The resulting powder mixture was compacted in a Perkin Elmer® manual hydraulic press at 10 Tm·cm^{-2} for 10 min. The spectrum of a KBr pellet containing approximately the same mass of KBr as the pellets of the ACs, was used as background. The FT-IR spectra registered for ACs prepared by the methods of physical and chemical activation are plotted in Fig. 1(a) and (b), respectively.

As far as the Boehm's method is concerned, the titration of various acidic oxygen surface groups and structures was performed using 0.05 M $NaHCO_3$ aqueous solution for carboxylic acid groups and carboxylic acid anhydrides, 0.05 M Na_2CO_3 for lactones and lactols, 0.05 M NaOH for phenolic hydroxyl groups, and 0.25 M NaOH for acidic carbonyl groups. Corrections were introduced in measured titration volumes by allowing that a base of a given strength is able to neutralize those surface functional groups and structures which are more acidic [46]. The values of contents of oxygen surface groups obtained for the prepared ACs are given in Table 3.

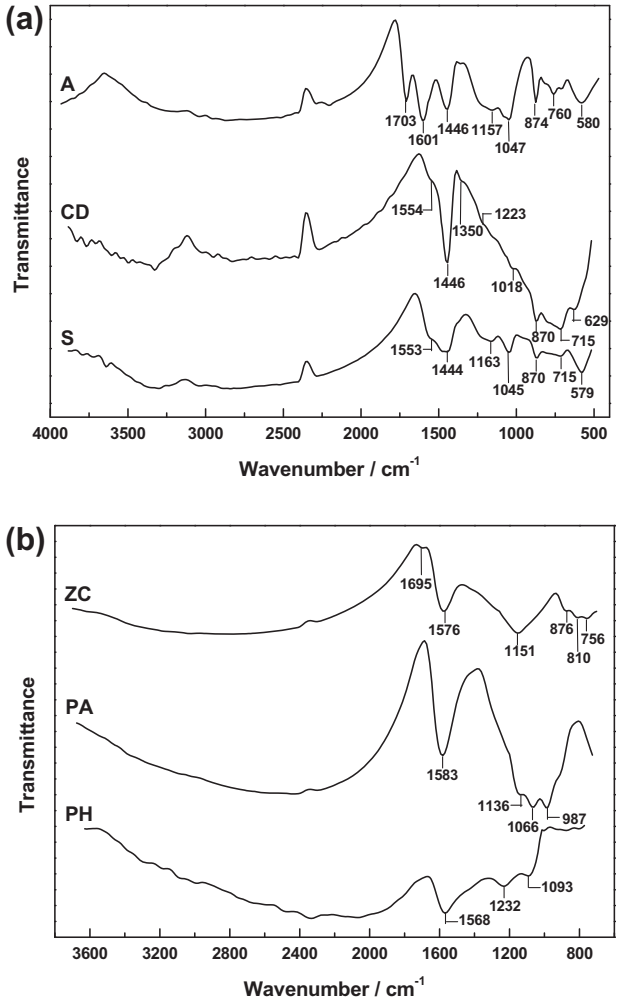

Fig. 1. FT-IR spectra of ACs prepared by the methods of physical (a) and chemical (b) activation.

Table 3
Surface chemistry of ACs. Content of oxygen surface groups.[a]

Sample	Oxygen surface groups and structures (meq g^{-1})				
	Carboxylic	Lactone	Phenolic hydroxyl	Carbonyl	Total
A	1.40	0.28	0.87	19.34	21.89
CD	1.91	n-m	0.10	10.10	12.11
S	0.77	0.15	n-m	9.33	10.25
PA	0.22	0.11	0.13	0.98	1.44
PH	0.17	0.79	n-m	1.37	2.33
ZC	0.24	n-m	n-m	1.25	1.49

[a] n-m: non-measureable.

2.3. Study of temperature dependence of dc electrical conductivity

In order to study the temperature dependence of the dc electrical conductivity (σ), the ACs were compressed into circular pellets with a total mass of around 200 mg, 13.2 mm in diameter and a variable thickness ranging from 1.0 to 3.0 mm. In the preparation of such pellets, each sample in a series of successive steps was oven-dried at 110 °C overnight, size-reduced for homogenization, accurately weighed, and thoroughly mixed with powder polyvinylidene fluoride (PVDF, Aldrich®) as binder, at the 80–20 wt.% ratio, in a small size agate mortar. After that, the resulting homogeneous powdery mixture was placed in a Perkin Elmer® manual hydraulic press and compacted at 10 Tm cm^{-2} for 3 min with the aid of a vacuum pump. Prior to carrying out the electrical conductivity measurements, the as-prepared pellets were stored in a desiccator to prevent the adsorption of gases and vapors from the laboratory atmosphere. As seen in Fig. 2, each pellet was placed inside a hollow alumina cylinder between two platinum foils forming the electrodes, the upper one movable and the lower one fixed, to get ohmic contact. The hollow cylinder was kept inside a vertical tubular furnace. A K-type thermocouple, whose hot junction is located close to the pellet, was used to accurately monitor the temperature during the measurements. The system was heated from room temperature up to ca. 200 °C in air atmosphere at a heating rate of 10 °C min^{-1} and, then, it was allowed to cool down to room temperature under the same atmosphere. The dc electrical resistance was recorded at different temperatures by the four-probe method [47–49], using a digital multimeter (Agilent®, model 34401A) connected to the electrodes. Since the conduction was considered to be ohmic in nature, the electrical conductivity was given by the following expression [50]:

$$\sigma = \frac{l}{R \cdot A} \tag{1}$$

where R is the electrical resistance in Ω, A the area of the pellet surface in cm^2, and l the thickness of the pellet in cm. The resistance of the platinum electrodes was verified and found to be at around 0.38 Ω, much lower than those of the samples under study.

3. Results and discussion

3.1. Carbonized products

Fig. 3 shows the variation of electrical conductivity with temperature for samples C600 and C900. It is seen first that conductivity increases with temperature for both carbonized products, being a typical feature of semiconductor materials [51]. Also, one observes that conductivity increases by three orders of magnitude as the carbonization temperature rises from 600 to 900 °C, which is in good agreement with the results previously obtained for a variety of lignocellulosic materials carbonized at similar temperatures, including rice husk [40] and straw [52], oil palm fiber [53], bamboo [54], lignin [55], woods [56–59], and so forth. The variation of conductivity with increasing heat treatment temperature may be explained on the basis of the chemical decomposition, degree of

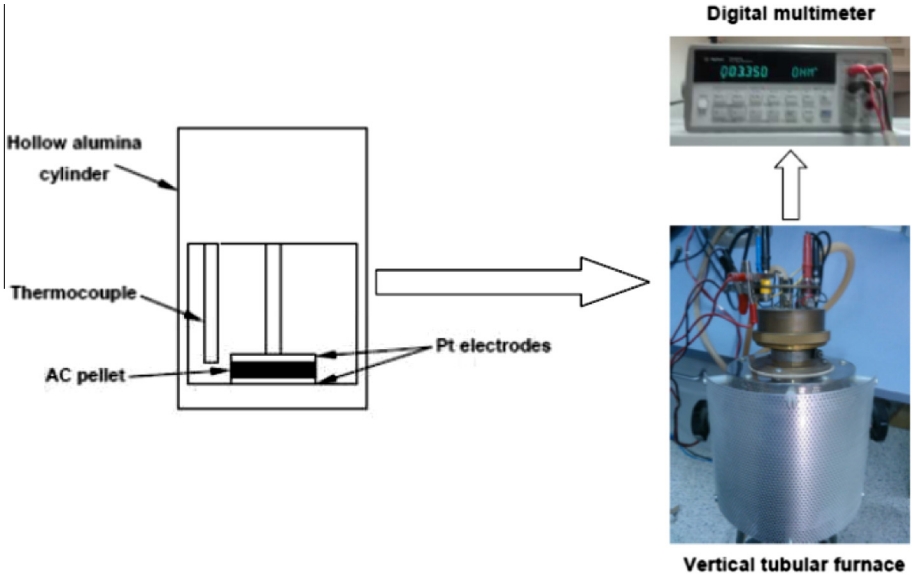

Fig. 2. Experimental device used for the measurement of the temperature-dependent dc electrical conductivity.

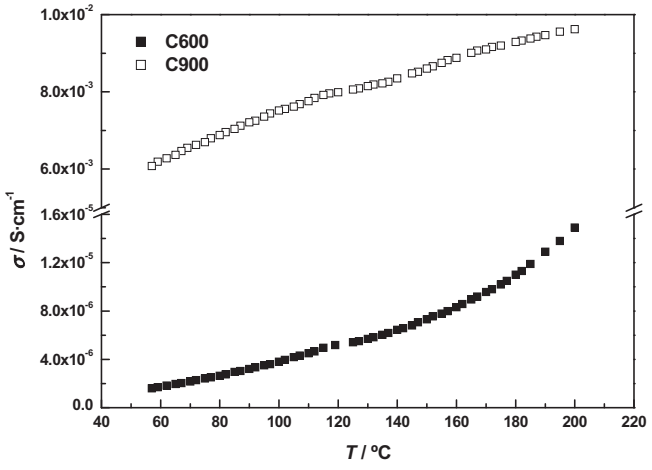

Fig. 3. Temperature dependence of the dc electrical conductivity for carbonized products.

conversion to carbon and microstructural evolution of VS components during the carbonization, as seen below.

Regarding the chemical composition of VS, significant differences were not observed between VS belonging to four varieties and two growing systems, being the average contents: holocellulose (i.e. cellulose + hemicellulose) 67.14%, lignin 20.27%, and ash 3.49% [60]. Since cellulosic materials are the main components (more than two thirds), it becomes apparent that their thermal decomposition largely determines the conversion of VS into carbon during the pyrolytic process as well as the properties of the resulting carbonized products, including their electrical conductivity. In this regard, Rhim et al. [61] have recently identified five regions of variation of conductivity as a function of heat treatment temperature during the carbonization of microcrystalline cellulose. At early stages of thermal treatment, between 250 and 350 °C, conductivity decreases with temperature due to the loss of polar oxygen-containing functional groups from cellulose molecules. Then, conductivity starts increasing with heat treatment temperature up to 500 °C as a result of the formation and growth of highly conductive carbon nano-clusters. At 600 °C, conductivity continues to increase as the nano-clusters grow in size and are close enough to each other to allow electron hopping and tunnelling between them [58]. A sharp increase of conductivity is observed in the range from 610 to 1000 °C due to percolation and the improvement of intrinsic conductivity of the carbon clusters. Finally, at higher temperatures up to 2000 °C, conductivity reaches a plateau and remains almost constant with increasing carbonization temperature [61,62]. This plateau has also been observed in the conductivity of other heat treated carbon materials [63–65].

The above-described behavior is consistent with the electrical conductivities measured for carbonized samples C600 and C900. According to Ruíz-Fernández et al. [9], the pyrolysis of VS is almost complete at 600 °C. The resulting carbonized product is mainly made up of carbon atoms arranged in turbostratic microcrystallites [65–68], which are embedded in a matrix of low conductive amorphous carbon, typically observed for other carbonized organic materials [61]. Such turbostratic microcrystallites are very small in size and too far away to allow effective electrical conduction by electron hopping and tunnelling between them, thus resulting in a very poor conductivity for sample C600. The subsequent slight decrease in mass as a result of rising the heat treatment temperature up to 900 °C is likely attributable to a small loss of heteroatoms, mainly hydrogen, increasing the C/H atomic ratio in C900 and thereby its degree of aromatization [9]. Mrozowski [65,68] proposed the following explanation for the steady increase in conductivity with increasing aromatization. As hydrogen atoms are released from the edge of graphene layers, some of the σ-electrons belonging to carbon atoms which were bounded to hydrogen are left unpaired. Some of these atoms become bonded to neighboring aromatic rings, increasing the size of the graphene layers. In the case of carbon atoms remaining unpaired, a π-electron is able to jump from the π-band into the σ-state, forming a spin pair and creating a hole at the top of the π-band. As a result, a large number of holes, i.e. positive charge carriers, are created and this accounts for the great increase in conductivity with increasing carbonization temperature.

As previously shown by Hernández et al. [63] and Emmerich et al. [64] for heat treated carbon materials, changes in porosity occurring during the carbonization process should also be taken into account to explain the bulk electrical conductivities of the

resulting carbonized materials. The products of VS carbonization have a very low development of micro and mesoporosity, being essentially macroporous solids (see Table 2). In addition, pore shrinkage occurs as heat treatment temperature rises from 600 to 900 °C [9] since V_T' is reduced from 0.62 $cm^3\ g^{-1}$ for C600 to 0.46 $cm^3\ g^{-1}$ for C900. A similar decrease in porosity at high carbonization temperatures has been reported elsewhere [69–71], and associated with lateral growth and improvement in planarity of graphene layer planes due to the aforesaid release of hydrogen [72]. Therefore, it becomes apparent that not only the increasing aromatization degree but also the decrease in porosity for sample C900 contribute to its much greater electrical conductivity (up to three orders of magnitude) as compared to C600. In this regard, it should be noted that the overall resistivity of granular and powder carbon materials is largely a function of the matter-free space in the sample. Such space comprises both the interparticle voids and the porosity corresponding to the intraparticle voids [49]. Therefore, the electrical conductivity should decrease as the total pore volume increases.

It is well known that the temperature dependence of the electrical conductivity for semiconductor materials can be expressed by the following Arrhenius-type equation [51,73]:

$$\sigma = \sigma_0 \cdot \exp\left(-\frac{E_g}{2k_B T}\right) \quad (2)$$

where E_g is the energy gap associated with electron hopping between conductive sites [61,65,74–76], k_B the Boltzmann's constant, T the temperature, and σ_0 denotes a constant whose value only depends on the material properties but not on the temperature [51]. Obviously, the factor $2k_BT$ must exceed the E_g value in order to electrical conduction takes place. The above equation can be expressed linearly as follows:

$$\ln \sigma = \ln \sigma_0 - \frac{E_g}{2k_B T} \quad (3)$$

Accordingly, if the carbon material exhibits semiconductor behavior, the plot of ln σ against T^{-1} should give a linear curve, and E_g may be estimated from the slope of the corresponding fitted line.

Fig. 4 depicts the plots of ln σ versus T^{-1} for the carbonized samples C600 and C900. One observes that the plots give nearly straight lines, which is the typical dependence of intrinsic semiconductors. For such materials, the variation of conductivity with temperature is mainly associated to the change in the number of charge carriers [65]. Experimental data shown in Fig. 4 have been fitted to Eq. (3) and the results are gathered in Table 4. It is seen that the data fit quite well this equation, R^2 values being higher than 0.99. The energy gap (E_g) decreases from 0.392 to 0.084 eV as heat treatment temperature increases from 600 to 900 °C, in very good agreement with the results previously reported for other carbonized materials [40,61,65,73,77–79].

Table 4
E_g values estimated for carbonized products and ACs samples.

Sample	E_g (eV)	R^2
C600	0.392	0.9967
C900	0.084	0.9945
A	0.659	0.9991
CD	0.107	0.9972
S	0.123	0.9950
PA	0.309	0.9972
ZC	0.455	0.9988
PH	0.121	0.9943

3.2. Activated carbons (ACs)

3.2.1. ACs prepared by physical activation

Fig. 5 shows the variation of conductivity with temperature for ACs prepared from VS by physical activation in air, CO_2 and steam. The plots for the carbonized products C600 and C900 have also been included in the above figure for comparison purposes. From this figure, it follows that physically activated samples also behave as semiconductor materials as their electrical conductivities increase with temperature. In addition, conductivity varies in the order: C900 ≈ S > CD ≈ C600 >> A over a wide temperature range. Since conductivity values are rather similar for samples C900 and S, it becomes apparent that the conductivity of the former is not significantly affected after its physical activation in steam. Conversely, activation of C600 and C900 with air and CO_2, respectively, results in ACs with lower electrical conductivities as compared to their corresponding carbonized substrata.

Regarding textural data, S_{BET}, W_0, V_{me} and V_T' are higher as follows: S > A > CD, therefore being steam the most effective activating agent to create porosity in the carbonized product (see Table 2). Since the presence of pores in the carbon samples acts as electrical

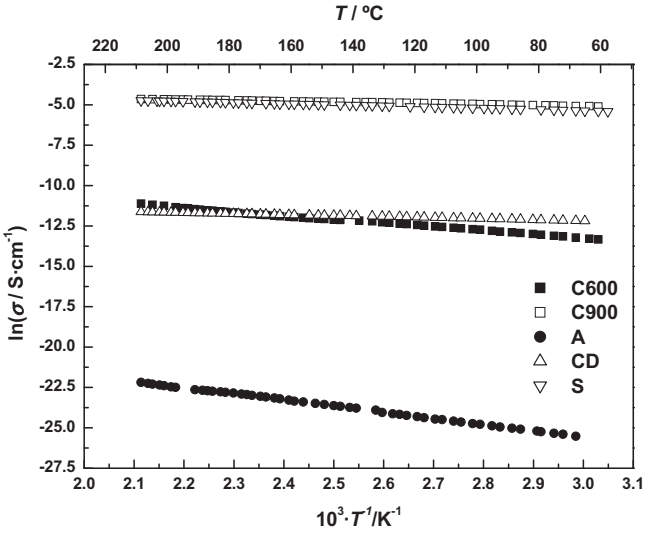

Fig. 4. Arrhenius-type plot of ln σ versus T^{-1} for carbonized products and ACs prepared by physical activation.

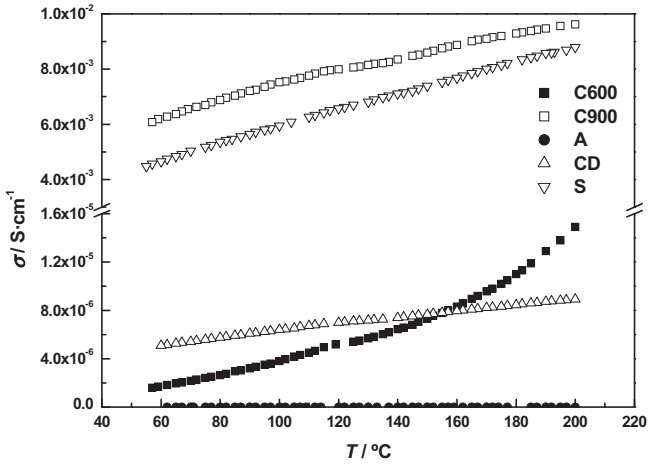

Fig. 5. Temperature dependence of the dc electrical conductivity for ACs prepared by physical activation.

resistance, as noted above, electrical conductivity should decrease with increasing V_T'. However, conductivity is found to increase in the order: S > CD >> A. Therefore, neither the extent of surface area nor the porosity of the ACs are the predominant factors determining the magnitude of their electrical conductivity. The divergence between both variation sequences for conductivity and porosity is likely attributable to other factors significantly influencing the electrical properties of the ACs, such as their chemical composition and surface chemistry.

As far as surface chemistry is concerned, a few previous works have shown that the electrical conductivity of carbon materials, including carbon blacks and activated carbons, is strongly dependent on their surface chemistry [78–80] and as a rule increases with decreasing concentration of surface functional groups [78,80], especially those containing oxygen and sulfur [81]. In this connection, it has been suggested that the activation with CO_2 leaves in the structure of the resulting ACs a larger amount of oxygen surface groups and structures as compared to steam [9,82–84]. Moreover, the ability of air to promote the formation of the aforesaid oxygen complexes in carbonized products during the activation stage is expected to be much higher than those for CO_2 and steam mainly due to the strong oxidizing character of the oxygen molecule, more pronounced at higher temperatures. Accordingly, the concentration of surface oxygen groups and structures in samples prepared by physical activation should be higher in the order A $\gg$ CD > S, which is in line with the variation observed for the conductivity of such ACs. The above sequence for the increasing concentration of oxygen complexes has been corroborated by using FT-IR spectroscopy [85] and by applying the Boehm's method. As shown in Fig. 1(a), the spectra registered for ACs prepared by physical activation display a great number of absorption bands, which are frequently strong. The spectrum of A exhibit a strong peak at 1703 cm^{-1} due to stretching (ν)(C=O) vibrations in carboxylic acid and quinone type structures. The bands at 1601 and 1446 cm^{-1} are attributable to ν(C=C) skeletal vibrations in aromatic rings. The two bands centred at 1157 and 1047 cm^{-1} may be assigned to ν(C—O—C) vibrations in ether type structures. Finally, low intensity bands at 874, 760 and 580 cm^{-1} may be related to C—H vibrations in substituted aromatic rings. In the CD and S spectra, a smaller number of less intense bands are observed, and no bands ascribable to the ν(C=O) vibration are registered. Accordingly, both the variety and concentration of oxygen surface groups and structures are higher in A as compared to CD and S. This latter assertion is well in agreement with the results obtained for the concentration of oxygen surface groups by the Boehm's method. As seen in Table 3, sample A is characterized by possessing a much higher total content of surface groups (21.89 meq g^{-1}) than for samples CD and S (12.11 and 10.25 meq g^{-1}, respectively). Concerning sample A, its contents of carboxylic acid, lactone and phenolic hydroxyl groups are low, whereas the content of carbonyl groups is markedly greater in the material. Furthermore, as compared to A, the contents of the various oxygen surface groups are substantially lower both for CD and S. It is particularly true for the phenolic hydroxyl and carbonyl groups. As the only exception to the rule, the concentration of carboxylic acid groups is slightly higher for CD (1.91 meq g^{-1}) than for A (1.40 meq g^{-1}). Therefore, in contrast to the activation with air, CO_2 and steam do not enhance the creation of most oxygen surface groups, except carbonyl ones. An explanation for the detrimental effect of surface oxides on the electronic properties of ACs was proposed by Smeltzer and McIntosh [86]. They suggested that the formation of functional groups on activated carbon by means of the reaction of oxygen with electron donating carbon atoms on the surface gives rise to an increasing localization of the conduction electrons and hence to a decreasing electrical conductivity.

The plots of ln σ against T^{-1} for ACs prepared by physical activation are illustrated in Fig. 4, together with those for C600 and C900. Similarly to carbonized products, these carbon samples also behave as intrinsic semiconductors and the experimental data are fitted very well by Eq. (3), the values of the determination coefficient (R^2) being higher than 0.99. The energy gap values estimated for these ACs are listed in Table 4. As shown in this table, the physical activation of the carbonized materials in air, CO_2 and steam results in significant changes not only in the magnitude of the conductivity but also in the energy gap associated with electron conduction. Indeed, the E_g values for the resulting ACs are higher as compared to their corresponding carbonized substrata, irrespective of the activating agent. Thus, the activation of C600 in air leads to an increase of E_g from 0.392 to 0.659 eV, while the effect is weaker for the activation of C900 with CO_2 and steam, E_g increasing from 0.084 to 0.107 and 0.123 eV, respectively. Therefore, it becomes apparent that the physical activation in air, CO_2 and steam strongly modifies the electronic band structure of the carbonized products from VS by increasing the band gap. Once again, such an effect of band gap widening might be associated with the formation of surface oxygen complexes during the activation stage in the process of preparation of ACs. Obviously, the increase in E_g is larger for sample A than for CD and S because of the greater oxidizing character of air as compared to CO_2 and steam.

3.2.2. ACs prepared by chemical activation

The variation of conductivity with temperature for ACs prepared from VS by chemical activation with H_3PO_4, $ZnCl_2$ and KOH is depicted in Fig. 6. Similarly to carbonized products and ACs prepared by physical activation, chemically activated samples also behave as semiconductors as their electrical conductivities increase with temperature. Moreover, conductivity is higher as follows: PH >> PA > ZC over the entire temperature range. This variation sequence may be explained by taking into account the differences in both texture and surface chemistry for the ACs as a result of the performance of the three activating agents in the preparation process.

As shown in Table 2, textural parameters for ACs prepared by chemical activation are larger than those obtained for physically activated samples. S_{BET}, W_0, V_{me} and V_T' vary in the order ZC > PA > PH, whereas V_{ma} is higher by PH > PA > ZC. Therefore, it becomes apparent that by the method of chemical activation ACs exhibiting a well-developed porosity in the three regions of pore sizes are prepared. As expected, such a porosity development has

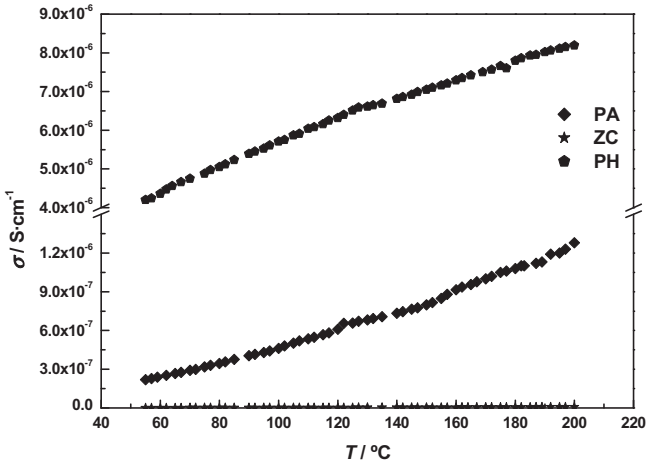

Fig. 6. Temperature dependence of the dc electrical conductivity for ACs prepared by chemical activation.

a detrimental effect on conductivity, which is as a rule lower for chemically activated samples as compared to their counterparts prepared by physical activation. In this regard, an excellent correlation has been observed between both variation sequences for conductivity and total pore volume for samples PH, PA and ZC.

Concerning chemical composition and surface chemistry, it should be noted that the conductivity of ACs prepared by chemical activation may be strongly affected by the presence in the samples of heteroatoms coming from the activating agent. In this connection, a number of works have proved the presence of a variety of phosphorous-containing groups and structures in ACs prepared from lignocellulosic waste products by chemical activation with H_3PO_4, including phosphate esters [13,86–91]. As previously reported by Bedia et al. [90], the amount of surface phosphorous in ACs prepared from olive stones by chemical activation with H_3PO_4 may be significant, ranging from 2 to 6 wt.% depending on both the impregnation ratio and the carbonization temperature. These authors found that the amount and stability of phosphorous incorporated to the carbon matrix increased with impregnation ratio and heat treatment temperature, respectively. Because of sample PA was prepared by using a H_3PO_4:VS impregnation ratio of 5:1 and by heating at 500 °C, it is evident that may have a relevant phosphorous content. Such an assertion is corroborated from the spectrum registered for PA (see Fig. 1(b)), which exhibits some strong absorption bands or shoulders ascribable to various P—O bond stretching modes, as follows: 1136 cm^{-1}, ν(P═O) in phosphates and ν(P—O—C); 1066 cm^{-1}, $\nu(P^+—O^-)$ in acid phosphate esters and ν_s(P—O—P) in polyphosphate chain; 987 cm^{-1}, ν(P—O) [13,90,91]. Similarly to carbon–oxygen complexes, the presence of phosphorous-containing groups and structures on carbon surface increases electronic localization and disrupts the π-conjugation, thus resulting in an increasing electrical resistance. An attempt of testing the influence of phosphorous on the electrical behavior of AC cloths prepared by chemical activation with various phosphorous-containing activating agents, such as phosphoric acid, sodium and potassium dihydrogen phosphate, and so on, has been recently reported by Ramos et al. [92,93]. They found that the electrical resistivity of the AC cloths was strongly dependent not only on the nature of the activating agent but also on the micropore volume and aromatization degree (i.e. the C/H atomic ratio). However, no paper dealing with the influence of phosphorous content on the electrical conductivity of ACs has been found. Therefore, it becomes apparent the need for further investigations aimed at clarifying the role of such an element on the electrical properties of ACs. On the other hand, the FT-IR spectra of PH and ZC display a number of absorption bands and shoulders which are assigned to various bond stretching vibration modes in atomic groups and structures, such as: 1576 and 1568 cm^{-1}, ν(C═C) in aromatic rings; 1232, 1151 and 1093 cm^{-1}, ν(C—O) in ether type structures. It should be noted that a weak band ascribable to the ν(C═O) vibration is only registered in the spectrum of ZC. Finally, as compared to the spectra of physically activated samples (see Fig. 1(a)), the spectra of those chemically activated show a smaller number of absorption bands. Therefore, it becomes apparent that the concentration of surface functional groups and structures is much lower in the ACs prepared by chemical activation. This latter assertion is also corroborated from the results obtained for the concentration of oxygen surface groups and structures (see data in Table 3).

In brief, from the above results it can be concluded that the magnitude of the electrical conductivity for ACs prepared by the method of chemical activation is largely controlled by the well-developed porosity rather than by the surface chemistry.

Fig. 7 shows the temperature-dependent electrical conductivity as an Arrhenius-type plot for ACs prepared from VS by the method of chemical activation. These carbon samples also exhibit the typical semiconductor behavior described by Eq. (3), with values of R^2 above 0.99. The energy gap values estimated for these ACs by fitting experimental data to the aforesaid equation are collected in Table 4. It is seen that the band gap widely varies depending on the activating agent and by the following order: PH (0.121 eV) < PA (0.309 eV) < ZC (0.455 eV).

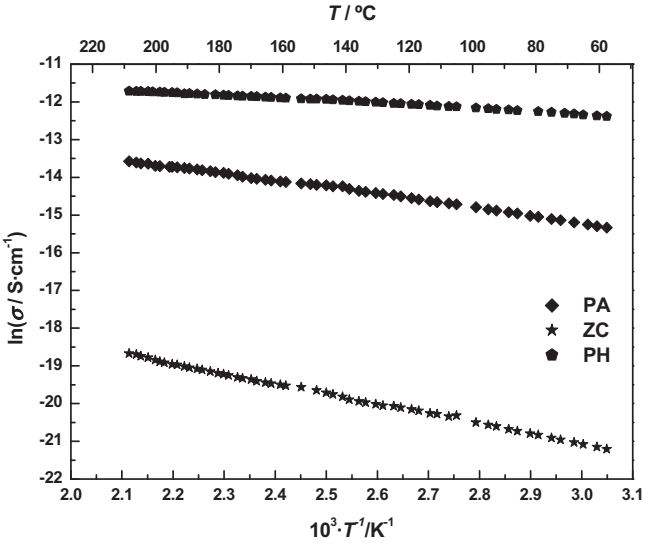

Fig. 7. Arrhenius-type plot of $\ln\sigma$ versus T^{-1} for ACs prepared by chemical activation.

Table 5
E_g values estimated for selected carbon materials.

Carbon material	E_g (eV)	References
Graphene	0	[97]
Crystalline graphite	0.04	[97,98]
Fullerenes	1.80	[97,99]
Activated carbons	0.05–0.2	[39,40]
Amorphous carbons	1–4	[100–105]

3.3. Comparison with other ACs and carbon materials

Table 5 collects the energy gap values estimated by theoretical calculations and experimental techniques, mainly optical and electrical measurements, for a wide range of carbon allotropic forms and materials, including graphene, graphite, activated and amorphous carbons, and so on. The E_g values estimated for ACs prepared in the present work are well in agreement with those previously reported for other activated carbons. As expected, the so-called turbostratic structure proposed for activated carbons, and consisting of aromatic sheets highly disorganized [94] and weakly bonded by van der Waals forces, leads to E_g values intermediate between those estimated for crystalline graphite (i.e. 0.04 eV) and amorphous carbons (from 1 to 4 eV). In addition, it should be mentioned that the relatively small E_g values determined for most activated carbons, and thereby their semiconductor properties, have been recently identified as responsible for the photocatalytic activity exhibited by these carbon materials in aqueous solution under UV irradiation [95,96].

4. Conclusions

The bulk electrical conductivity of various ACs prepared from VS by the method of physical activation in air, CO_2 and steam, and by the method of chemical activation with H_3PO_4, $ZnCl_2$ and

KOH is found to be the result of a complex interplay between several factors. Among them, texture and surface chemistry seem to be the more relevant. The physical activation has been proved to decrease the electrical conductivity of the carbonized products, the reduction being more pronounced in the order: air > CO_2 > steam. Such a detrimental effect on conductivity is likely connected with the formation of oxygen groups and structures on carbon surface during the activation stage rather than with the porosity development. Conversely, the higher degree of porosity development accounts for the low conductivity values measured for ACs prepared by chemical activation, the effect of surface chemistry being of less significance. In this case, both porosity and conductivity varies by KOH < H_3PO_4 < $ZnCl_2$. The temperature-dependent electrical conductivity measurements suggest that both carbonized products and ACs behave as typical semiconductor materials, regardless the activation method and activating agent. Consequently, the electrical conduction process is associated with an energy gap, which has been found to widely vary from 0.084 eV for the VS carbonized at 900 °C up to 0.659 for the AC prepared by physical activation in air atmosphere.

Acknowledgements

Financial support by Gobierno de Extremadura and European FEDER Funds is gratefully acknowledged. A. Barroso-Bogeat thanks Spanish Ministerio de Educación, Cultura y Deporte for the concession of a FPU grant (AP2010-2574).

References

[1] H. Marsh, F. Rodríguez-Reinoso, Activated Carbon, Elsevier, Amsterdam, 2006.
[2] F. Rodríguez-Reinoso, in: F. Schüth, K.S.W. Sing, J. Weitkamp (Eds.), Handbook of Porous Solids, Wiley-VCH, GmBh, Weinham, 2002, p. 1766.
[3] R.C. Bansal, J.B. Donnet, F. Stoeckli, Active Carbon, Marcel Dekker, New York, 1988.
[4] M. Olivares-Marín, J.A. Fernández, M.J. Lázaro, C. Fernández-González, A. Macías-García, V. Gómez-Serrano, F. Stoeckli, T.A. Centeno, Mater. Chem. Phys. 114 (2009) 323–327.
[5] H. Jankowska, A. Swiatkowski, J. Choma, Active Carbon, Ellis Horwood, New York, 1991.
[6] F. Rodríguez-Reinoso, in: H. Marsh, E.A. Heintz, F. Rodríguez-Reinoso (Eds.), Introduction to Carbon Technologies, Universidad de Alicante, Alicante, 1997, pp. 35–101.
[7] T.J. Bandosz, Activated Carbon Surfaces in Environmental Remediation, Elsevier, Amsterdam, 2006.
[8] J.M. Dias, M.C.M. Alvim-Ferraz, M.F. Almeida, J. Rivera-Utrilla, M. Sánchez-Polo, J. Environ. Manage. 85 (2007) 833–846.
[9] M. Ruíz-Fernández, M. Alexandre-Franco, C. Fernández-González, V. Gómez-Serrano, Adsorption 17 (2011) 621–629.
[10] L. Jiménez-Alcaide, F. López-Baldovin, I. Sánchez-Parra, J.L. Ferrer, Rev. ATIP 46 (1992) 85–88.
[11] Junta de Extremadura, Consejería de Agricultura y Medioambiente, 2002.
[12] A. Melgar, A. Diego, M. Lapuerta, J.J. Hernández, A. Alkassir, Energía 51 (2003) 5–6.
[13] B. Corcho-Corral, M. Olivares-Marín, C. Fernández-González, V. Gómez-Serrano, A. Macías-García, Appl. Surf. Sci. 252 (2006) 5961–5966.
[14] P.A.M. Mourão, C. Laginhas, F. Custódio, J.M.V. Nabais, P.J.M. Carrott, M.M.L. Ribeiro-Carrott, Fuel Process. Technol. 92 (2011) 241–246.
[15] J.M. Valente-Nabais, C. Laginhas, P.J.M. Carrott, M.M.L. Ribeiro-Carrott, J. Anal. Appl. Pyrolysis 87 (2010) 8–13.
[16] M. Ruíz-Fernández, M. Alexandre-Franco, C. Fernández-González, V. Gómez-Serrano, Sci. Technol. 28 (2010) 751–759.
[17] B. Corcho-Corral, M. Olivares-Marín, E. Valdés-Sánchez, C. Fernández-González, A. Macías-García, V. Gómez-Serrano, J. Agric. Food Chem. 53 (2005) 644–650.
[18] P. Serp, J.L. Figueiredo, Carbon Materials for Catalysis, Wiley, New Jersey, 2009.
[19] E. Frackowiak, F. Béguin, Carbon 39 (2001) 937–950.
[20] A.G. Pandolfo, A.F. Hollenkamp, J. Power Sources 157 (2006) 11–27.
[21] A. Burke, Electrochim. Acta 53 (2007) 1083–1091.
[22] A. Davies, A. Yu, Can. J. Chem. Eng. 89 (2011) 1342–1357.
[23] A. Ghosh, Y.H. Lee, ChemSusChem 5 (2012) 480–499.
[24] L. Wei, G. Yushin, Nano Energy 1 (2012) 552–565.
[25] W. Lei, X. Zhao, P. He, H. Liu, Chem. Bull. 76 (2013) 981–987.
[26] J. Wang, S. Kaskel, J. Mater. Chem. 22 (2012) 23710–23725.
[27] F. Béguin, E. Raymundo-Piñero, E. Frackowiak, in: F. Béguin, E. Frackowiak (Eds.), Carbons for Electrochemical Energy Storage and Conversion Systems, CRC Press, Boca Ratón, 2010, pp. 329–376.
[28] Y. Zhai, Y. Dou, D. Zhao, P.F. Fulvio, R.T. Mayes, S. Dai, Adv. Mater. 23 (2011) 4828–4850.
[29] Y.P. Wu, E. Rahm, R. Holze, J. Power Sources 114 (2003) 228–236.
[30] J.C. Arrebola, A. Caballero, L. Hernán, J. Morales, M. Olivares-Marín, V. Gómez-Serrano, J. Electrochem. Soc. 157 (2010) A791–A797.
[31] P. Kalyani, A. Anitha, Int. J. Hydrogen Energy 38 (2013) 4034–4045.
[32] X. Peng, J. Fu, C. Zhang, J. Tao, L. Sun, P.K. Chu, Nanosci. Nanotechnol. Lett. 6 (2014) 68–71.
[33] P. Novák, D. Goers, M.E. Spahr, in: F. Béguin, E. Frackowiak (Eds.), Carbons for Electrochemical Energy Storage and Conversion Systems, CRC Press, Boca Ratón, 2010, pp. 263–328.
[34] M. Zhi, C. Xiang, J. Li, M. Li, N. Wu, Nanoscale 5 (2012) 72–88.
[35] L.L. Zhang, Y. Gu, X.S. Zhao, J. Mater. Chem. A 1 (2013) 9395–9408.
[36] J. Sánchez-González, F. Stoeckli, T.A. Centeno, J. Electroanal. Chem. 657 (2011) 176–180.
[37] P.J. Hall, M. Mirzaeian, S.I. Fletcher, F.B. Sillars, A.J.R. Rennie, G.O. Shitta-Bey, G. Wilson, A. Cruden, R. Carter, Energy Environ. Sci. 3 (2010) 1238–1251.
[38] B. Viswanathan, P. Indra Neel, T.K. Varadarajan, Methods of Activation and Specific Applications of Carbon Materials, National Centre for Catalysis Research, Indian Institute of Technology Madras, Chennai, 2009.
[39] W.M. Daud, M. Badri, H. Mansor, J. Appl. Phys. 67 (1990) 1915–1917.
[40] L. John Kennedy, J. Judith Vijaya, G. Sekaran, Mater. Chem. Phys. 91 (2005) 471–476.
[41] E. Pollak, I. Genish, G. Salitra, A. Soffer, L. Klein, D. Aurbach, J. Phys. Chem. B 110 (2006) 7443–7448.
[42] A. Subrenat, J.N. Baléo, P. Le Cloirec, P.E. Blanc, Carbon 39 (2001) 707–716.
[43] S. Brunauer, P.H. Emmet, E. Teller, J. Am. Chem. Soc. 60 (1938) 309–319.
[44] M.M. Dubinin, in: J.F. Danielli, M.D. Rosenberg, D.A. Cadenhead (Eds.), Progress in Surface and Membrane Science, vol. 9, Academic Press, New York, 1975, pp. 1–70.
[45] H.P. Boehm, Carbon 32 (1994) 759–769.
[46] J. Jaramillo, P.M. Álvarez, V. Gómez-Serrano, Fuel Process. Technol. 91 (2010) 1768–1775.
[47] K.J. Euler, J. Power Sources 3 (1978) 117–136.
[48] A. Espinola, P.M. Miguel, M.R. Salles, A.R. Pinto, Carbon 24 (1986) 337–341.
[49] J. Sánchez-González, A. Macías-García, M.F. Alexandre-Franco, V. Gómez-Serrano, Carbon 43 (2005) 741–747.
[50] S. Mrozowski, Proceedings third Biennal Carbon Conference, Pergamon Press, Buffalo, 1957. p. 495.
[51] W.D. Callister, Introducción a la Ciencia e Ingeniería de los Materiales, Ed. Reverté, Barcelona, 1996.
[52] G. Xiao, R. Xiao, B. Jin, W. Zuo, J. Liu, J.R. Grace, J. Biobased Mater. Bioenergy 4 (2010) 426–429.
[53] N. Indayaningsih, A. Zulfia, D. Priadi, S. Hendrana, Adv. Mater. Res. 277 (2011) 137–142.
[54] Z.H. Jiang, D.S. Zhang, B.H. Fei, Y.D. Yue, X.H. Chen, New Carbon Mater. 19 (2004) 249–253.
[55] X. Xu, G. Xiao, J. Cao, J. Southeast Univ. 43 (2013) 115–119.
[56] T. Manabe, M. Ohata, S. Yoshizawa, D. Nakajima, S. Goto, K. Uchida, H. Yajima, Trans. Mater. Res. Soc. Jpn. 32 (2007) 1035–1038.
[57] J.H. Kwon, S.B. Park, N. Ayrilmis, S.W. Oh, N.H. Kim, Composites Part B 46 (2013) 102–107.
[58] A.K. Kercher, D.C. Nagle, Carbon 40 (2002) 1321–1330.
[59] H. Sugimoto, M. Norimoto, Carbon 42 (2004) 211–218.
[60] L. Jiménez, V. Angulo, E. García, A. Rodríguez, Afinidad 61 (2004) 194–203.
[61] Y.-R. Rhim, D. Zhang, D. Howard, Carbon 48 (2010) 1012–1024.
[62] A.G. Dumanli, A.H. Windle, J. Mater. Sci. 47 (2012) 4236–4250.
[63] J.C. Hernández, I. Hernández-Calderón, C.A. Luengo, R. Tsu, Carbon 20 (1982) 201–205.
[64] F.G. Emmerich, J.C. de Sousa, I.L. Torriani, C.A. Luengo, Carbon 25 (1987) 417–424.
[65] H.T. Pinnick, Proceedings of the First Conference on Carbon, American Carbon Society, New York, 1956, pp. 3–11.
[66] O. Paris, C. Zollfrank, G.A. Zickler, Carbon 43 (2005) 53–66.
[67] A.K. Kercher, D.C. Nagle, Carbon 41 (2003) 15–27.
[68] S. Mrozowski, Phys. Rev. 85 (1952) 609–620.
[69] J.W. Neely, Carbon 19 (1981) 27–36.
[70] J. Pastor-Villegas, C. Valenzuela-Calahorro, A. Bernalte-García, V. Gómez-Serrano, Carbon 31 (1993) 1061–1069.
[71] V. Gómez-Serrano, J. Pastor-Villegas, C.J. Durán-Valle, Carbon 34 (1996) 533–538.
[72] K.J. Masters, B. McEnaney, Carbon 22 (1984) 595–601.
[73] P.L. Walters, Proceedings of the Fifth Carbon Conference, vol. II, Pennsylvania State University, 1961, p. 131.
[74] A.W.P. Fung, M.S. Dresselhaus, M. Endo, Phys. Rev. B 48 (1993) 14953–14962.
[75] C. Godet, S. Kumar, V. Chu, Philos. Mag. 83 (2003) 3351–3365.
[76] C. Godet, Diam. Relat. Mater. 12 (2003) 159–165.
[77] Z.Q. Shi, Q.L. Qian, C.Y. Wang, S.F. Zhang, G.Q. Yuan, L. Wang, New Carbon Mater. 24 (2009) 314–320.
[78] S.S. Barton, J.E. Koresh, Carbon 22 (1984) 481–485.
[79] M. Polovina, B. Babić, B. Kaluderović, A. Dekanski, Carbon 35 (1997) 1047–1052.
[80] D. Pantea, H. Darmstadt, S. Kaliaguine, C. Roy, Appl. Surf. Sci. 217 (2003) 181–193.

[81] D. Pantea, H. Darmstadt, S. Kaliaguine, L. Sümmchen, C. Roy, Carbon 39 (2001) 1147–1158.
[82] F. Rodríguez-Reinoso, M. Molina-Sabio, M.T. González, Carbon 33 (1995) 15–23.
[83] M. Belhachemi, F. Addoun, E-J. Chem. 8 (2011) 992–999.
[84] M.T. González, M. Molina-Sabio, F. Rodríguez-Reinoso, in: Extended Abstracts 21st Biennial Conference on Carbon, Buffalo, New York, 1993, p. 416.
[85] M. Ruíz-Fernández, Preparation and characterization of activated carbon from vine shoots. Adsorption of methylene blue from aqueous solution, University of Extremadura, Badajoz, 2009.
[86] W.W. Smeltzer, R. McIntosh, Can. J. Chem. 31 (1953) 1239–1251.
[87] S. Somasundaram, K. Sekar, V.K. Gupta, S. Ganesan, J. Mol. Liq. 177 (2013) 416–425.
[88] M.S. Solum, R.J. Pugmire, M. Jagtoyen, F. Derbyshire, Carbon 33 (1995) 1247–1254.
[89] M. Jagtoyen, M.W. Thwaites, J.M. Stencel, B. McEnaney, F.J. Derbyshire, Carbon 30 (1992) 1089–1096.
[90] J. Bedia, R. Barrionuevo, J. Rodríguez-Mirasol, T. Cordero, Appl. Catal. B 103 (2011) 302–310.
[91] A.M. Puziy, O.I. Poddubnaya, A. Martínez-Alonso, F. Suárez-García, J.M.D. Tascón, Carbon 43 (2005) 2857–2868.
[92] M.E. Ramos, J.D. González, P.R. Bonelli, A.L. Cukierman, Ind. Eng. Chem. Res. 46 (2007) 1167–1173.
[93] M.E. Ramos, P.R. Bonelli, S. Blacher, M.M.L. Ribeiro-Carrott, P.J.M. Carrott, A.L. Cukierman, Colloids Surf. A 378 (2011) 87–93.
[94] F. Rodríguez-Reinoso, Carbon 36 (1998) 159–175.
[95] I. Velo-Gala, J.J. López-Peñalver, M. Sánchez-Polo, J. Rivera-Utrilla, Appl. Catal. B 142–143 (2013) 694–704.
[96] L.F. Velasco, I.M. Fonseca, J.B. Parra, J.C. Lima, C.O. Ania, Carbon 50 (2012) 249–258.
[97] R. Sanjinés, M.D. Abad, C. Vâju, R. Smajda, M. Mionić, A. Magrez, Surf. Coat. Technol. 206 (2011) 727–733.
[98] N. García, P. Esquinazi, J. Barzola-Quiquia, S. Dusari, New J. Phys. 14 (2012) 053015.
[99] E.E. Kohnke, J. Phys. Chem. Solids 23 (1962) 1557–1562.
[100] S.H. Moustafa, M. Koós, I. Pócsik, J. Non Cryst. Solids 227–230 (1998) 1087–1091.
[101] S. Bhattacharyya, S.R.P. Silva, Thin Solid Films 482 (2005) 94–98.
[102] A. Tibrewala, E. Peiner, R. Bandorf, S. Biehl, H. Lüthje, Appl. Surf. Sci. 252 (2006) 5387–5390.
[103] M. Doyama, A. Ichida, Y. Inoue, Y. Kogure, T. Nozaki, S. Yamada, Scr. Mater. 44 (2001) 1191–1194.
[104] B. Meyerson, F.W. Smith, J. Non Cryst. Solids 35–36 (1980) 435–440.
[105] J.J. Hauser, J. Non Cryst. Solids 23 (1977) 21–41.